JOURNAL OF VIROLOGY, Aug. 2007, p. 8579–8586 Vol. 81, No. 16
0022-538X/07/$08.00+0 doi:10.1128/JVI.00263-07

A Protein Kinase A-Dependent Mechanism by Which Rotavirus Affects the Distribution and mRNA Level of the Functional Tight Junction-Associated Protein, Occludin, in Human Differentiated Intestinal Caco-2 Cells[▽]

Isabelle Beau,[1,2]† Jacqueline Cotte-Laffitte,[1,2]† Raymonde Amsellem,[1,2] and Alain L. Servin[1,2]*

INSERM, UMR 756, Châtenay-Malabry, France,[1] *and Faculté de Pharmacie, Université Paris-Sud, Châtenay-Malabry, France*[2]

Received 7 February 2007/Accepted 24 May 2007

We found that at the tight junctions (TJs) of Caco-2 cell monolayers, rhesus monkey rotavirus (RRV) infection induced the disappearance of occludin. Confocal laser scanning microscopy showed the disappearance of occludin from the cell-cell boundaries without modifying the expression of the other TJ-associated proteins, ZO-1 and ZO-3. Western immunoblot analysis of RRV-infected cells showed a significant fall in the levels of the nonphosphorylated form of occludin in both Triton X-100-insoluble and Triton X-100-soluble fractions, without any change in the levels of the phosphorylated form of occludin. Quantitative reverse transcription-PCRs revealed that the level of transcription of the gene that encodes occludin was significantly reduced in RRV-infected cells. Treatment of RRV-infected cells with Rp-cyclic AMP and protein kinase A inhibitors H89 and KT5720 during the time course of the infection restored the distribution of occludin and a normal level of transcription of the gene that encodes occludin.

Rotaviruses are nonenveloped, double-stranded RNA viruses belonging to the *Reoviridae* family. Although rotavirus can infect older children and adults, diarrheal disease caused by rotaviruses is seen mainly in children under 2 years of age. Mortality rates are low in developed countries, where the illness is usually self-limiting, but in contrast, in developing countries throughout the world more than 600,000 young children die each year. These viruses exhibit a marked tropism for the differentiated enterocytes of the intestinal epithelium (38, 54). Over the last 10 years, an increasing number of studies using the enterocyte-like model of Caco-2 cells have provided new insights into the pathophysiological mechanisms by which rotaviruses induce structural and functional damage in intestinal cells without causing any apparent cell destruction (12, 58). For example, rhesus rotavirus (RRV) induces Ca^{2+}-dependent rearrangements in brush border-associated proteins, including the microvillar proteins F-actin and villin (9, 10). The activity and expression of sucrase-isomaltase (SI) at the brush border of intestinal cells are specifically and selectively reduced by a mechanism dependent on a cyclic-AMP (cAMP)-dependent protein, protein kinase A (PKA), that leads to the blockade of the direct transportation of SI from the trans-Golgi network to the brush border without affecting the biosynthesis, maturation, or stability of the enzyme (30, 41). In addition, rotavirus can induce lesions in the tight junctions (TJs) of monolayer-forming, polarized epithelial cells. In monolayers of Madin-Darby canine kidney (MDCK) cells, the rotavirus outer capsid protein VP8, a trypsin-cleaved product of the rotavirus VP4 protein, was capable of inducing a dose-dependent and reversible change in the fence function of TJs, thus opening the paracellular space normally sealed by the TJs (46). The long-term exposure of MDCK-1 cell monolayers to the rotavirus nonstructural NSP4 protein causes a reversible reduction in transepithelial electrical resistance and an increase in the paracellular passage of fluorescein isothiocyanate (FITC)-dextran (61). RRV infection of Caco-2 cell monolayers is followed by dramatic lesions in the TJs characterized by a progressive, postinfection time-dependent decrease in transepithelial resistance and an increase in paracellular permeability accompanied by rearrangements of the distribution of TJ-associated proteins (17, 49).

In the intestine, epithelial cells are physically linked by intercellular junctional complexes. TJs, which are located on the uppermost basolateral surface of polarized enterocytes, regulate diffusion between cells and allow the epithelia to form a cellular barrier separating the external and internal compartments (42). The intercellular gate formed by TJs is not only highly regulated but is size and ion selective and therefore constitutes a semipermeable diffusion barrier that forms a morphological and functional boundary between the apical and basolateral cell surface domains. TJs also contribute directly to maintaining cell surface polarity by forming a fence that prevents the apical-basolateral diffusion of lipids and proteins. The elements constituting TJs have been classified as proteins that span the cytoplasmic membrane and cytoplasmic proteins, thus linking these membrane proteins to the cytoskeleton (24). The peripheral junctional proteins, members of the membrane-associated guanylate kinase (MAGuK) family of proteins comprising the zonula occludens 1 (ZO-1), ZO-2, and ZO-3 proteins (25, 26, 60), play a particular role in the organization of the TJs (23). ZO-1 can bind directly to ZO-2 or ZO-3 to form ZO-1/ZO-2 and ZO-1/ZO-3 complexes, and it establishes a link with the actin cytoskeleton by interacting directly with actin filaments. As a result, ZO-1 binds directly to

* Corresponding author. Mailing address: Faculté de Pharmacie, INSERM Unit 510, Châtenay-Malabry, France 92296. Phone: 33 1 46 83 56 61. Fax: 33 1 46 83 58 44. E-mail: alain.servin@u-psud.fr.
† I. Beau and J. Cotte-Laffitte contributed equally to this work.
▽ Published ahead of print on 6 June 2007.

the cytoplasmic tail of occludin, thus linking the transmembrane protein occludin and the actin cytoskeleton. This allows the formation of heteromeric complexes, including occludin, ZO-2, and ZO-3. ZO-1, ZO-2, and ZO-3 all also interact with claudins. Moreover, the TJ-associated proteins that play a major role in the functions of TJs include the transmembrane proteins occludin (22) and the claudins (21). In particular, occludin contributes to the electrical barrier function of the TJs and plays a pivotal role in regulating the paracellular barrier function (18, 43). Our group has previously reported that RRV infection of Caco-2 cells leads to rearrangements of occludin at the TJs (49). The aim of our experiments was to identify the mechanism by which RRV induces rearrangements of occludin.

MATERIALS AND METHODS

Antibodies and reagents. The rabbit polyclonal anti-ZO1 (clone Z-R1), rabbit polyclonal anti-ZO3 (clone ZMD.261), and mouse monoclonal anti-occludin (clone OC-3F10) antibodies were supplied by Zymed (Invitrogen, Cergy, France). Polyclonal anti-rotavirus antibody was from Agrobio (La Ferté St Aubin, France). Rabbit polyclonal anti-actin antibody was from Sigma (Sigma-Aldrich Chimie SARL, L'Isle d'Abeau Chesnes, France). FITC- and tetramethyl rhodamine isothiocyanate-conjugated secondary antibodies were from Jackson (Interchim, Montluçon, France). All other reagents were of superior analytical grade.

The anti-protease cocktail used (leupeptin, aprotinin, antipain, benzamidine, pepstatin A, phenylmethylsulfonyl fluoride), trypsin, paraformaldehyde, H89, and Triton X-100 were purchased from Sigma. Gö6976, Rp-cAMP, KT5720, and Ro318220 were purchased from Calbiochem (VWR International, Fontenay sous Bois, France).

Virus. The RRV stock used was generated in MA104 cells after preincubating the cells for 3 h in a serum-free culture medium (30). Viruses were activated by treatment with 0.5 μg/ml trypsin at 37°C for 30 min, and MA104 cell monolayers were infected at a multiplicity of infection of 0.01. After being left to adsorb for 1 h at 37°C, the inoculum was removed and the infected cells were incubated in serum-free medium containing 0.5 μg/ml trypsin. After a complete cytopathic effect had been obtained, the cultures were frozen and then thawed and the cell debris was removed by centrifugation.

Semipurified virus was prepared as described by Cuadras et al. (16). Briefly, RRV-infected MA104 cells were harvested after a complete cytopathic effect was attained, the cell extracts were pelleted through a 4-ml cushion of 50% sucrose in minimal Eagle's medium buffer by centrifugation for 2 h at 26,000 rpm at 4°C.

Genetic inactivation of RRV was accomplished as previously described, through a process using psoralen and long-wavelength UV light that irreversibly cross-links viral RNA but does not alter the hemagglutination function or antigenic characteristics of RRV proteins (9). Briefly, 2 ml of a virus suspension was mixed with 4′-aminomethyl-4,5′,8-trimethylpsoralen at 20 μg/ml in a petri box (30-mm diameter) and incubated at 4°C for 15 min. Virus was then exposed to UV light at 366 nm for 40 min. The petri box was placed on ice, and the distance between the surface of the suspension and the light source was 2 cm. The effectiveness of psoralen-UV inactivation was demonstrated by the lack of detectable viral antigen in an immunofluorescence assay in MA104 cells infected with psoralen-UV-treated RRV (data not shown).

Preparation of culture supernatants of RRV-infected Caco-2 cells. After 22 h of infection, culture supernatants of RRV-infected cells were centrifuged at 100,000 × *g* for 3 h. To eliminate proteins with molecular masses of up to 50 kDa, supernatants were then filtered with Amicon filters with a 50-kDa cutoff (Millipore, Molsheim, France). The lack of infectious virus in the treated culture supernatants was verified with MA104 cells.

Cell cultures. The parental Caco-2 cell line was used for cell cultures (19, 51). Cells (passages 60 to 90) were routinely grown in Dulbecco modified Eagle's minimal essential medium with 25 mM glucose (Life Technologies, Cergy, France) supplemented with 15%, heat-inactivated (30 min, 56°C) fetal calf serum (FCS; Life Technologies) and 1% nonessential amino acids (Life Technologies, Cergy, France) as previously described. For maintenance purposes, the cells were passaged weekly with 0.02% trypsin in Ca^{2+}- and Mg^{2+}-free phosphate-buffered saline (PBS) containing 3 mM EDTA. Experiments and maintenance of the cells were carried out at 37°C in a 10% CO_2–90% air atmosphere. The culture medium was changed daily. For assays of rotavirus infection, Caco-2 cells were used at postconfluence after 14 days of culture (i.e., they were fully differentiated cells).

MA104 cells were cultured in minimum Eagle's medium supplemented with 10% FBS, 1% glutamine, antibiotics (20 U/ml penicillin, 40 U/ml streptomycin), and 1% nonessential amino acids in a 5% CO_2 incubator. Cells (10^5/cm^2) were seeded in 150-cm^2 tissue culture flasks (Falcon; Becton-Dickinson, Le Pont-de-Claix, France) and were used for virus production and virus titer determination (30).

Infection conditions. The method used for Caco-2 cell infection has been described elsewhere (30). Briefly, a virus inoculum was activated for 30 min by exposure to 0.5 μg/ml trypsin. Caco-2 cells cultured without FCS for 24 h were apically infected with an inoculum of activated RRV at a multiplicity of infection of 10 for 1 h at 37°C. The inoculum was then removed, and fresh medium containing 0.5 μg/ml trypsin was added. Infected cells were incubated at 37°C in an atmosphere containing 10% CO_2–90% air. All assays were conducted at 18 h postinfection. Each assay was performed by three successive passages of Caco-2 cells.

Cell integrity was confirmed by measuring the lactate dehydrogenase (LDH) activity in the apical compartment of filter-grown cells (Enzyline LDH kit; BioMérieux, Dardilly, France) according to the manufacturer's instructions. The LDH release measured in control H_2O-lysed cells was taken as the 100% value. Results were expressed as milliunits of LDH activity per milligram of protein assayed by the bicinchoninic acid assay. No significant release of LDH was observed during the time for which the cells were examined for experiments, indicating that no cell lysis had occurred.

Immunofluorescence detection of TJ-associated proteins. For direct or indirect immunofluorescence labeling, cultured cells were prepared on glass coverslips, which were then placed in 24-well TPP tissue culture plates (ATGC, Marne la Vallée, France).

For detection of TJ-associated proteins, cells were fixed in 3% paraformaldehyde in PBS (pH 7.4) for 15 min at room temperature and then treated with 50 mM NH_4Cl for 10 min. Monolayers were permeabilized with 0.2% Triton X-100 in PBS for 4 min at room temperature and then washed twice with PBS and saturated for 1 h with PBS containing 0.2% gelatin and 10% FCS. Primary antibodies were diluted in 0.2% gelatin in PBS (anti-ZO-1, anti-ZO-3, and anti-occludin at a dilution of 1:200 each). The coverslips were then incubated with primary antibodies for at least 2 h, washed three times in PBS–0.2% Tween, and then incubated with the appropriate secondary FITC- or tetramethyl rhodamine isothiocyanate-conjugated secondary antibodies (at a dilution of 1:100) for at least 1 h.

The cells were incubated for 10 min with DABCO antifading reagent (Dako-Cytoformation, Trappes, France), and the coverslips were mounted in Glycergel (DakoCytoformation). Specimens were examined by epifluorescence microscopy with a confocal laser scanning microscope (Zeiss LSM 510 equipped with an air-cooled 488-nm argon ion laser and a 543-nm helium neon laser) configured with an Axiovert 100 M microscope with a Plan Apochromat 63×/1.40 oil objective. Optical sectioning was used to collect 50 en face images 0.1 μm apart. Horizontal views were obtained by integrating images obtained with a step position of 1 with the accompanying Zeiss software (LSM510 2.5) in Windows NT4. Photographic images were resized, organized, and labeled with Adobe Photoshop software (Adobe, San Jose, CA).

Western blot analysis. For preparation of Triton X-100-soluble and -insoluble protein fractions, the cells were washed once with cold PBS and then treated for 15 min at 4°C with Triton X-100 extraction buffer (25 mM HEPES, 0.5% Triton X-100, 150 mM NaCl, 2 mM EDTA) containing protease inhibitors (phenylmethylsulfonyl fluoride, 10 μg/ml aprotinin, 10 μg/ml leupeptin, 10 μg/ml pepstatin, 4 mM sodium orthovanadate, 40 mM sodium fluoride). The resulting supernatant was collected and considered the Triton X-100-soluble fraction. The cells were then scraped into the same volume of extraction buffer and referred to as the Triton X-100-insoluble fraction. The protein concentration of each sample was quantified by the Bradford method. The fractions were dissolved in the appropriate volume of Laemmli buffer and held at 100°C for 5 min. Proteins were separated by 8% sodium dodecyl sulfate-polyacrylamide gel electrophoresis (SDS-PAGE). For Western blot analysis, the proteins were electrotransferred onto a polyvinylidene difluoride membrane (Perkin-Elmer, Les Ullis, France). The polyvinylidene difluoride membranes were then incubated with anti-occludin, anti-ZO-1, anti-ZO-3, and anti-actin primary antibodies at dilutions of 1:500, 1:200, and 1/1,000, respectively. A goat anti-rabbit or anti-mouse horseradish peroxidase-linked antibody (Amersham, Orsay, France) was used at a 1/10,000 dilution as a secondary antibody. Bound immunoglobulins were revealed by the ECL+ detection system under conditions recommended by the manufacturer (Amersham, Orsay, France).

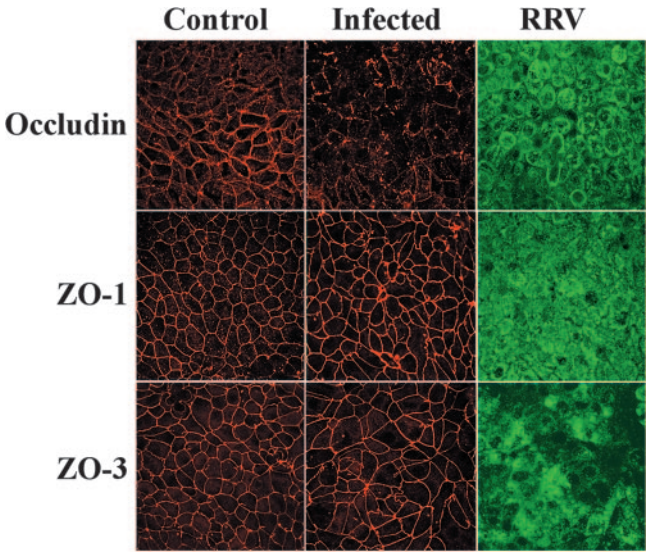

FIG. 1. Rearrangement of the distribution of occludin, but not that of ZO-1 and ZO-3, in RRV-infected Caco-2 cells. Fully differentiated cells were left uninfected or were infected with RRV for 18 h. The cells were permeabilized and processed for indirect immunofluorescence labeling of occludin, ZO-1, ZO-3, and rotavirus proteins as described in Materials and Methods. All images were obtained by confocal laser scanning microscopy. Micrographs are representative of three independent experiments.

Quantitative reverse transcription-PCR (Q-RT-PCR). Total RNA was isolated from control and RRV-infected Caco-2 cells with the TRIzol total RNA isolation reagent (Invitrogen Life Technologies, Cergy-Pontoise, France). First-strand cDNA was generated by RT of 5 μg of total RNA with random hexamers and the Superscript III RT kit (Invitrogen Life Technologies, Cergy-Pontoise, France).

Real-time PCR was performed with a Light Cycler thermal cycler (Roche Diagnostics, Meylan, France). To quantify the genes for occludin and glyceraldehyde-3-phosphate dehydrogenase (GAPDH), we used the Fast Start DNA MasterPLUS SYBR green I Master Mix (Roche Diagnostics, Meylan, France) with each primer at 300 nM. The sequences of the oligonucleotide primers used were as follows: occludin, 5′-AAGCAAGTGAAGGGATCTGC-3′ and 5′-GGGGTTATGGTCCAAAGTCA-3′; GAPDH, 5′-CAGCCTCAAGATCATCAGCA-3′ and 5′-TGTGGTCATGAGTCCTTCCA-3′. To quantify the ZO-1 gene, we used the Quantitec SYBR green PCR Master Mix with the QuantiTec Primer assay (QT00077308; (QIAGEN SA, Courtaboeuf, France). Dissociation curves were generated after each Q-RT-PCR run to ensure that a single specific product was amplified. Threshold cycle (C_t) values were calculated by using the second derivative maximum algorithm provided by the Light Cycler software. Five serial dilutions of cDNA were analyzed for each target gene and used to construct linear standard curves. All PCR efficiencies (E), calculated from the slopes of the calibration curves according to the equation $E = [10^{-(1/\text{slope})}] - 1$, were above 90%. To compensate for variations in the RNA input and in the efficiency of the Q-RT-PCR, we used a normalization strategy based on the housekeeping gene for GAPDH. The raw data for the expression of occludin and ZO-1 were divided by the quantity of GAPDH present to obtain the normalized value of the yield expressed in arbitrary units.

All experiments were carried out in triplicate, with each data point representing a separate culture. The experiments yielded similar results each time.

Treatment with inhibitors. Rp-cAMP (20 μM), a combination of the PKA inhibitors H89 (10 μM) and KT5720 (10 μM), the mitogen- and stress-activated protein kinase 1 (MSK1) inhibitor Ro31822 (5 μM), or the PKC Ca^{2+}-dependent inhibitor Gö6976 (10 μM) was added to the culture medium during the infection time course.

Statistics. Data are expressed as the mean ± the standard error of the mean of several experiments, with at least three monolayers from three successive passages of cells per experiment. Statistical significance was assessed by a Student t test.

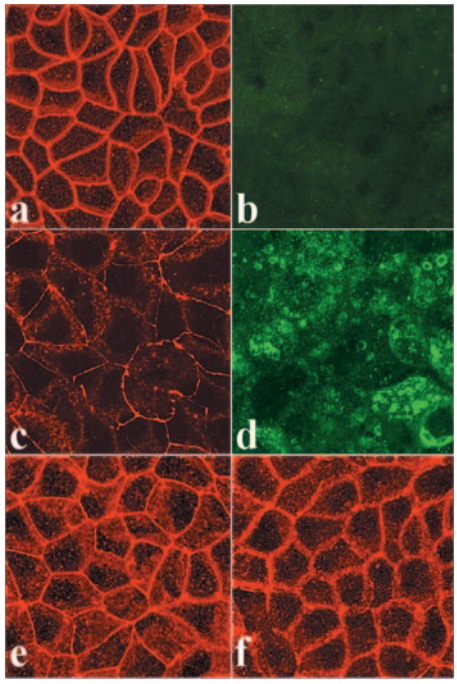

FIG. 2. Effect of purified RRV, UV-inactivated RRV, and culture supernatants of RRV-infected Caco-2 cells on the distribution of occludin in Caco-2 cells. Fully differentiated noninfected cells are shown in panels a and b. In panels c to g, cells were infected with purified RRV (c and d) or UV-inactivated virus (e) for 18 h or exposed for 1 h to supernatants of RRV-infected cells that had been cleared of infectious virus and of proteins with molecular masses of up to 50 kDa by filtration (f). The cells were permeabilized and processed for indirect immunofluorescence labeling of occludin or rotavirus proteins as described in Materials and Methods. All images were obtained by confocal laser scanning microscopy. Micrographs are representative of three independent experiments.

RESULTS

Occludin disappears from TJs in RRV-infected cells. Occludin expression was observed by confocal laser scanning microscopy analysis. In uninfected control Caco-2 cells at postconfluence, forming the typical sharp, honeycomb-like organization of fully differentiated cultured human intestinal cells, occludin was located, as usual, at cell-cell boundaries (Fig. 1). Occludin was located at the cell-to-cell contact between uninfected control cells, and some of the proteins had been distributed into the cytoplasm. The distribution of occludin was dramatically modified in RRV-infected cells; the change was characterized by a marked depletion of the protein from the plane of the TJs (Fig. 1). Moreover, when occludin remained TJ associated in randomly distributed areas, the staining seemed to be discontinuous, in contrast to the continuous staining seen in uninfected control cells. In order to demonstrate that the change in occludin in RRV-infected cells was specific, immunolocalization of TJ-associated proteins ZO-1 and ZO-3 was conducted. Figure 1 shows that ZO-1 and ZO-3 were distributed normally in RRV-infected cells, as in uninfected control cells, forming a brightly stained continuous band lining every cell. An identical result was obtained with a purified virus (Fig. 2c). Moreover, no change in occludin expression was observed when Caco-2 cells were infected with psoralen-UV-inactivated RRV, indi-

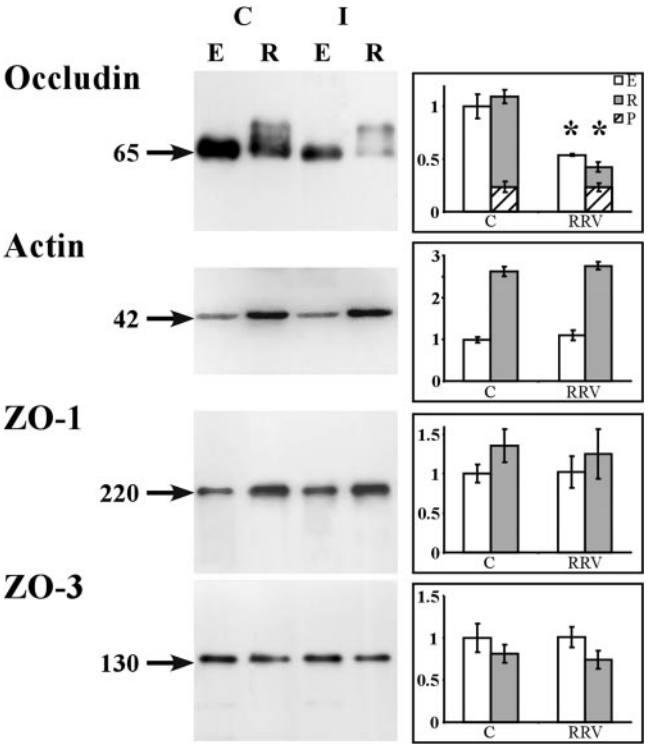

FIG. 3. Decrease in the occludin contents of Triton X-100-soluble and -insoluble fractions isolated from RRV-infected Caco-2 cells. Fully differentiated cells were left uninfected or were infected with RRV for 18 h. The cells were processed for isolation of Triton X-100-soluble and -insoluble fractions. Detergent-insoluble and -soluble fractions were resolved by SDS-PAGE and Western immunoblotted for detection of occludin, ZO-1, and ZO-3 proteins as described in Materials and Methods. Representative immunoblot assays from three independent experiments are shown. (Left side) Immunoblot analysis of occludin and ZO-1 in the Triton X-100-soluble (E) and -insoluble (R) fractions of control (C) or RRV-infected (I) Caco-2 cells. Actin was used as a loading control for immunoblotting. Arrows indicate the 65-kDa nonphosphorylated occludin band, the 220-kDa ZO-1 band, the 130-kDa ZO-3 band, and the 42-kDa actin band. (Right side) Blots were quantified with NIH Image software. Open bars, nonphosphorylated form of occludin in Triton X-100-soluble fraction. Closed bars, nonphosphorylated form of occludin in Triton X-100-insoluble fraction. Hatched bars, phosphorylated (P) form of occludin in Triton X-100-insoluble fraction. For the nonphosphorylated form of occludin in the Triton X-100-soluble and -insoluble fractions, each bar represents the mean ± the standard deviation of three independent experiments. *, $P > 0.01$ (Student t test) compared with appropriate control cells.

cating that virus replication is required for the RRV-induced inhibitory effect (Fig. 2e).

The rotavirus NSP4 protein, which is released into culture supernatants of rotavirus-infected Caco-2 cells, has been found to be able to induce TJ lesions in Caco-2 cells (61). This prompted us to examine whether culture supernatants of RRV-infected Caco-2 cells trigger the changes in occludin expression described above. For this purpose, we exposed naive Caco-2 cells to the culture supernatants of RRV-infected Caco-2 cells that were cleared of infectious virus and from which proteins with molecular masses of up to 50 kDa were eliminated by filtration. As shown in Fig. 2f, the treated culture supernatants of RRV-infected cells were not able to promote the disorganization of occludin.

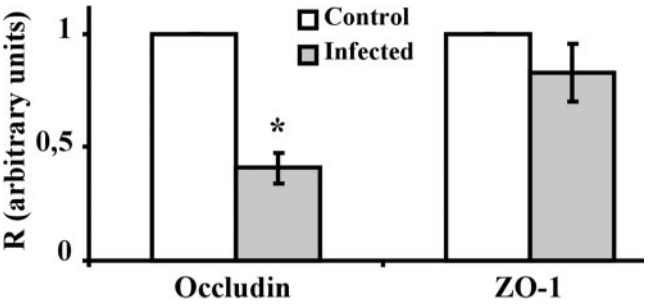

FIG. 4. Decrease in the occludin mRNA level in RRV-infected Caco-2 cells. Fully differentiated cells were left uninfected or were infected with RRV for 18 h. Total RNA was extracted, and the occludin and ZO-1 mRNAs were quantified by Q-RT-PCR. C_t values obtained for these two mRNA transcripts were normalized relative to those for GAPDH. Results are expressed as occludin/GAPDH and ZO-1/GAPDH ratios (R). Each bar represents the mean ± the standard deviation of three independent experiments. For occludin, $P < 0.01$ (Student t test) for the difference between RRV-infected cells and control cells. For ZO-1, the Student t test showed no significant difference between RRV-infected cells and control cells.

The decreased expression of occludin in RRV-infected cells reported above prompted us to examine the distribution of the protein in the Triton X-100-soluble and Triton X-100-insoluble fractions (Fig. 3). As a negative control, the distribution of ZO-1 and that of ZO-3 were examined in parallel. Western blot analysis of uninfected control cells showed that ZO-1, ZO-3, and occludin were expressed in the detergent-soluble fraction as single bands of 220 kDa, 130 kDa, and 65 kDa, respectively. In the detergent-insoluble fraction, ZO-1 and ZO-3 were detected as single bands of 220 kDa and 130 kDa, respectively, whereas occludin formed two bands, one of 65 kDa and a second of 72 kDa, corresponding to the nonphosphorylated and phosphorylated forms of the protein, respectively (57). Densitometric analysis revealed a 50 to 60% decrease in the levels of the nonphosphorylated form of occludin in both the detergent-soluble and detergent-insoluble fractions of the RRV-infected cells compared to those in uninfected control cells. In contrast, densitometric analysis showed that the level of the phosphorylated form of occludin in the detergent-insoluble fraction was the same in RRV-infected Caco-2 cells as in uninfected control cells. The densitometric analysis of the Western blots shows that for the ZO-1 and ZO-3 negative controls, the levels of the proteins in both the detergent-soluble and detergent-insoluble fractions isolated from RRV-infected cells were the same as those in uninfected control cells.

RRV reduces the level of occludin mRNA. RRV infection of Caco-2 cells resulted in changes in the levels of the nonphosphorylated form of occludin in both the detergent-soluble and detergent-insoluble fractions; this led us to wonder whether these altered protein levels were a consequence of the change in mRNA level. To find out, we used real-time Q-RT-PCR to determine the level of occludin mRNA in uninfected control and RRV-infected Caco-2 cells. Since no change in the expression and distribution of ZO-1 had been observed earlier, the level of ZO-1 transcripts was used as a negative control. As shown in Fig. 4, infection with RRV significantly reduced the occludin mRNA level compared to that in uninfected control

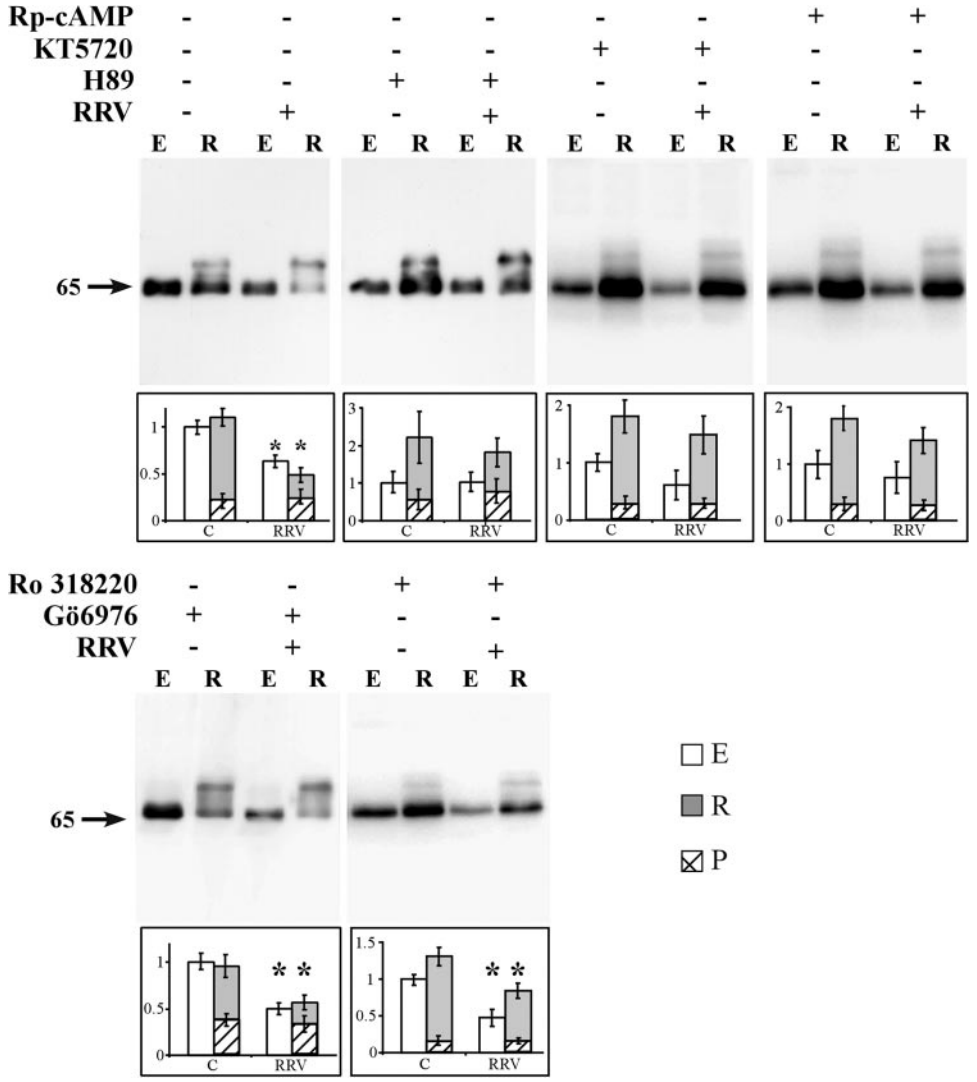

FIG. 5. Rp-cAMP and PKA inhibitors, but not PKC and MSK1 inhibitors, restore the expression of occludin in RRV-infected Caco-2 cells. Detergent-insoluble and -soluble fractions were resolved by SDS-PAGE and Western immunoblotted for detection of occludin as described in Materials and Methods. Representative immunoblot assays from three independent experiments are shown. Western blot analysis of occludin in the Triton X-100-soluble (E) and Triton X-100-insoluble (R) fractions of control (C) or RRV-infected (I) Caco-2 cells which had or had not been treated with Rp-cAMP, the PKA inhibitors H89 and KT5720, the MSK1 inhibitor Ro318220, or the PKC inhibitor Gö6976. The position of the 65-kDa form of nonphosphorylated occludin is indicated. Blots were quantified with NIH Image software. Open bars, nonphosphorylated form of occludin in Triton X-100-soluble fraction; closed bars, nonphosphorylated form of occludin in Triton X-100-insoluble fraction; hatched bars, phosphorylated (P) form of occludin in Triton X-100-insoluble fraction. Each bar represents the mean ± the standard deviation of three independent experiments. *, $P > 0.01$ (Student t test) compared with appropriate control cells.

cells. Consistent with the fact that RRV infection promotes no change in the expression or distribution of ZO-1, the mRNA level of ZO-1 was the same in RRV-infected cells as that in uninfected control cells.

PKA inhibitors reversed the RRV-induced loss of occludin. Among the various types of signaling proteins and signal transduction pathway transfer signals that modulate TJ assembly and functions, PKC and cAMP-dependent PKA have been shown to regulate several rearrangements of TJ-associated proteins (44). We investigated whether the PKC inhibitor Gö6976, the MSK1 inhibitor Ro318220, and/or the PKA inhibitors Rp-cAMP, H89, and KT5720 reverse the RRV-induced rearrangements of occludin. PKC inhibitor and PKA inhibitor treatments did not affect viral replication (log titers of RRV per well: control RRV, 6.81 ± 0.5; RRV plus H89, 6.68 ± 0.4; RRV plus Rp-cAMP, 6.53 ± 0.6; RRV plus KT5720, 6.75 ± 0.4; RRV plus Ro318220, 6.59 ± 0.6; RRV plus Gö6976, 6.41 ± 0.5). Moreover, all of the inhibitor treatments did not modify the virus infectivity and did not modify the expression and distribution of occludin in uninfected, nontreated cells (not shown). Western immunoblot assays and densitometric analysis showed that in the uninfected cells treated with the PKA inhibitor or PKC inhibitor, the levels of the phosphorylated or nonphosphorylated forms of occludin were not modified compared with those in uninfected, nontreated cells (Fig. 5). PKA inhibitor Rp-cAMP, KT5720, and

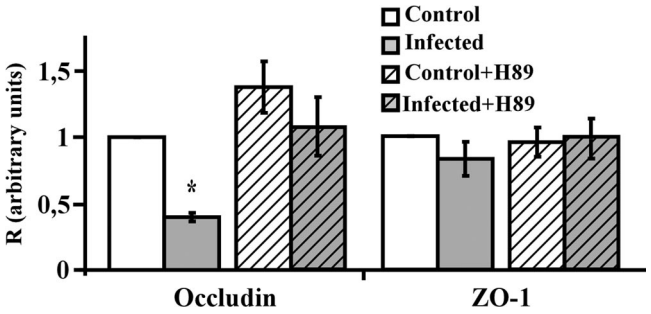

FIG. 6. PKA inhibitor reversed the RRV-induced fall in the occludin mRNA level in Caco-2 cells. Fully differentiated cells were left uninfected or were infected with RRV for 18 h, with or without the PKA inhibitor H89. Total RNA was extracted, and occludin mRNAs were quantified by Q-RT-PCR. C_t values obtained for occludin mRNA transcripts were normalized relative to those of GAPDH. Results are expressed as the TJs protein/GAPDH ratio (R). Each bar represents the mean ± the standard deviation of three independent experiments. *, $P > 0.01$ (Student t test) compared with RRV-infected or inhibitor-treated, RRV-infected cells.

H89 treatments reversed the RRV-induced decrease in the nonphosphorylated form of occludin. Indeed, in the PKA inhibitor-treated, RRV-infected cells, normal expression of the nonphosphorylated form of occludin was observed in both the detergent-soluble and detergent-insoluble fractions, compared with that in uninfected control cells. Considering that H89 also inhibits MSK1 (40), we have examined whether the MSK1 inhibitor Ro318220 antagonizes the RRV-induced changes in occludin distribution in RRV-infected cells. As shown in Fig. 5, MSK1 inhibitor Ro318220 treatment failed to restore the normal expression of occludin. Identically, PKC inhibitor Gö6976 treatment was not able to reverse the RRV-induced decrease in the nonphosphorylated form of occludin (Fig. 5).

Determining the level of occludin transcripts by Q-RT-PCR showed that the PKA inhibitor treatment inhibited the RRV-induced effect on the transcription of the occludin mRNA since the level of occludin mRNA was restored to a level identical to that in untreated, uninfected cells (Fig. 6). It was noted that the PKA inhibitor H89 treatment did not significantly affect the transcription of occludin mRNA in uninfected cells (Fig. 6). Moreover, the PKA inhibitor H89 treatment did not affect the transcription of ZO-1 mRNA in uninfected and RRV-infected cells (Fig. 5).

DISCUSSION

In previous studies, it has been reported that rotavirus infection promotes structural and functional changes in TJs of intestinal Caco-2 cells (17, 49) and MDCK cells (46, 61). Here, we describe for the first time the mechanism by which rotavirus affects the functional TJ-associated protein occludin by the demonstration that RRV affects occludin at the mRNA level in enterocyte-like Caco-2 cells. Occludin is a polytopic membrane protein that appears to span the membrane four times and to expose both of its termini to the cytosol (18, 22, 43). Occludin plays crucial roles in the formation of TJs and in regulating paracellular permeability (5, 6, 20). Enterovirulent bacterial pathogens that use sophisticated strategies involving virulence factors subverting host cell signaling pathways affect the architecture of TJs and in turn disrupt the TJ-associated regulatory functions controlling paracellular passage (8, 27). For example, *Clostridium difficile* toxins (11, 48) and cytotoxic necrotizing factor 1 from *Escherichia coli* have been shown to modify the organization of TJ-associated proteins (50). Enteropathogenic *E. coli* infection leads to the appearance of aberrant TJ strands in the lateral membrane of the intestinal epithelium (45). There are few reports about interactions between viruses and TJs. Exposing brain microvascular endothelial cells to human immunodeficiency virus type 1 Tat protein results in reduced expression and a change in the distribution of TJ-associated proteins (2). The mechanisms underlying these changes appear to be complex, since inhibitors of several signaling pathways partially prevent Tat-mediated changes in the claudin 5 protein. The adenovirus E4-ORF1 protein in MDCK cells blocked the TJ localization of ZO-2, as well as their interacting partners, and disrupted both the TJ barrier and apicobasal polarity (36). The coxsackievirus and adenovirus receptor (CAR), a 46-kDa integral membrane protein with a typical transmembrane region (7), which plays a pivotal role in the cell entry of group B coxsackievirus (14), has been found at TJs. CAR associates with ZO-1 (13) and multi-PDZ domain protein 1 (15) and forms part of the barrier to the movement of macromolecules and ions (13). However, it remains to be determined whether the interaction of coxsackievirus with TJ-associated CAR promotes any change in TJ-associated proteins and functions.

TJs constitute a highly regulated domain, since their assembly and permeability are regulated by signaling pathways involving calcium, cAMP, diacylglycerol, tyrosine kinases, heterodimeric G proteins, Ras and Rho GTP-binding proteins, PKC, and PKA (44). Examining the role of Ca^{2+}-dependent signaling, which plays a pivotal role in rotavirus pathogenicity (55), our group has previously reported that the RRV-induced, Ca^{2+}-dependent rearrangements of the apical cytoskeleton in Caco-2 cells does not correlate with the RRV-induced alteration of TJ-associated proteins (49). cAMP-dependent regulatory effects have been observed at the TJs of MDCK cells (32–34). A signaling cascade implicating the small GTPases Rab13 and PKA has been shown to be involved in the dynamics of TJ assembly (33). The results reported here demonstrate that the disappearance of occludin from the TJ plane, the fall in the levels of the nonphosphorylated form of occludin in both the detergent-soluble and detergent-insoluble fractions, and the decrease in occludin mRNA could be antagonized by PKA inhibitors. Similar PKA-dependent inhibition has been observed for the delocalization of occludin to the TJ plane by a calcium switch treatment (32). It should be noted that another PKA-dependent mechanism has been observed recently during rotavirus infection resulting in the inhibition of the intracellular transport of SI in RRV-infected Caco-2 cells (41).

Two forms of occludin have been characterized at TJs, a nonphosphorylated lower-molecular-weight form and a higher-molecular-weight form which is hyperphosphorylated. The phosphorylation and dephosphorylation of occludin are important for the organization and functionality of TJs (3, 31, 47, 57, 63). Dephosphorylation correlates with TJ dysfunction, and several enterovirulent bacteria, such as *Shigella flexneri* and enteropathogenic *E. coli*, induce intestinal barrier dysfunction by promoting a progressive shift of occludin from the plane of

the TJs through the dephosphorylation of occludin (56, 59). The mechanism by which RRV affects occludin is different. Indeed, in contrast to the results obtained with enterovirulent bacteria, no change in the hyperphosphorylated form of occludin was observed in RRV-infected Caco-2 cells.

There was a decrease in the nonphosphorylated form of the protein in both the detergent-soluble and detergent-insoluble fractions of RRV-infected Caco-2 cells. It has been reported that the loss of occludin in *Vibrio cholerae*-infected cells occurs because the *V. cholerae* hemagglutinin/protease cleaves occludin into two subfragments (64). This is not the case for RRV infection, since no occludin subfragment was observed by Western blotting in the RRV-infected cells, indicating that the RRV-induced disappearance of the nonphosphorylated form of occludin cannot have been due to protein degradation. The disappearance of the nonphosphorylated form of occludin was correlated with a marked reduction of occludin mRNA. This effect appears to be specific, since no change was observed in ZO-1 mRNA. As far as we are aware, this is the first time that a significant change in transcript levels of a TJ-associated protein has been reported to be linked to an enterovirulent microorganism in human intestinal cells. What is the mechanism by which RRV specifically affects the level of occludin mRNA? Direct repression of the expression of the gene for occludin has been reported following activation of the transcription factor Snail (28) or activation of the cellular protooncogene Raf-1 (37). Activation of Snail or Raf-1 results in the general down-regulation of TJ-associated proteins ZO-1, occludin, and claudins and of the adherens junction-associated protein E-cadherin. Our results were different since we observed that ZO-1 was not down-regulated, and our group has previously reported that E-cadherin was not modified upon RRV infection (49). One other possible hypothesis is that the virus or viral proteins could affect the stability of mRNAs. Another hypothesis is that the virus or viral proteins could affect the level of mRNAs coding for occludin by interfering with the transcription of the occludin gene. In general, cAMP signaling to the nucleus is accomplished by translocation of the catalytic subunit of PKA into the nucleus, where it phosphorylates and activates activating and silencing transcription factors, both of which can target responsive element sites present in a promoter. Upstream from the transcription start point for human occludin mRNA, a number of putative transcription factor binding sites have been described, including TCF, NF-interleukin-6, and AP2 (1, 62). Interestingly, some PKA-dependent regulation of the transcription factor AP2 has been reported. Indeed, follicle-stimulating hormone upregulates anti-Mullerian hormone expression through a nonclassical cAMP-PKA pathway involving the transcription factor AP2 (35). Ethanol- and isoproterenol-increased proenkephalin promoter activity results in PKA-dependent regulation of the proenkephalin promoter containing two cAMP response elements (CRE-1 and CRE-2) and one AP2 site (65). The increase in the transcriptional activity of nerve growth factor IC was abolished in the presence of the PKA inhibitor H89, indicating that a signaling transduction mechanism through PKA plays a role in nerve growth factor IC-induced, AP2-dependent transactivation (52). Direct negative regulation of AP2 by rotavirus remains to be demonstrated, but indirect down-regulation of AP2 by rotavirus could be hypothesized. Indeed, tumor necrosis factor alpha and gamma interferon can down-regulate the expression of occludin by diminishing occludin promoter activity (39). In rotavirus-infected pigs (4) and humans (29), these two cytokines have been found to be increased, and it was interesting that PKA-dependent down-regulation of cyclic nucleotide phosphodiesterase 3B at the protein and mRNA levels has been reported to be promoted by tumor necrosis factor alpha (53). Further studies will try to delineate the mechanism by which rotavirus or a rotavirus protein(s) negatively regulates the occludin promoter.

ACKNOWLEDGMENTS

We are grateful to V. Nicolas for assistance with confocal laser scanning microscopy and to C. Delomenie for assistance with Q-RT-PCR (IFR141, Faculté de Pharmacie Paris XI).

This work was supported by the French Ministère Délégué à la Recherche et aux Nouvelles Technologies, Programme de Microbiologie: Microbiologie fondamentale et appliquée, Maladies infectieuses, Environnement et bioterrorisme (grant ACIM-2-18, 2003-5 to A.L.S.).

REFERENCES

1. **Ando-Akatsuka, Y., M. Saitou, T. Hirase, M. Kishi, A. Sakakibara, M. Itoh, S. Yonemura, M. Furuse, and S. Tsukita.** 1996. Interspecies diversity of the occludin sequence: cDNA cloning of human, mouse, dog, and rat-kangaroo homologues. J. Cell Biol. **133:**43–47.
2. **Andras, I. E., H. Pu, J. Tian, M. A. Deli, A. Nath, B. Hennig, and M. Toborek.** 2005. Signaling mechanisms of HIV-1 Tat-induced alterations of claudin-5 expression in brain endothelial cells. J. Cereb. Blood Flow Metab. **25:**1159–1170.
3. **Andreeva, A. Y., E. Krause, E. C. Muller, I. E. Blasig, and D. I. Utepbergenov.** 2001. Protein kinase C regulates the phosphorylation and cellular localization of occludin. J. Biol. Chem. **276:**38480–38486.
4. **Azevedo, M. S., L. Yuan, S. Pouly, A. M. Gonzales, K. I. Jeong, T. V. Nguyen, and L. J. Saif.** 2006. Cytokine responses in gnotobiotic pigs after infection with virulent or attenuated human rotavirus. J. Virol. **80:**372–382.
5. **Balda, M. S., C. Flores-Maldonado, M. Cereijido, and K. Matter.** 2000. Multiple domains of occludin are involved in the regulation of paracellular permeability. J. Cell. Biochem. **78:**85–96.
6. **Bamforth, S. D., U. Kniesel, H. Wolburg, B. Engelhardt, and W. Risau.** 1999. A dominant mutant of occludin disrupts tight junction structure and function. J. Cell Sci. **112:**1879–1888.
7. **Bergelson, J. M., J. A. Cunningham, G. Droguett, E. A. Kurt-Jones, A. Krithivas, J. S. Hong, M. S. Horwitz, R. L. Crowell, and R. W. Finberg.** 1997. Isolation of a common receptor for coxsackie B viruses and adenoviruses 2 and 5. Science **275:**1320–1323.
8. **Berkes, J., V. K. Viswanathan, S. D. Savkovic, and G. Hecht.** 2003. Intestinal epithelial responses to enteric pathogens: effects on the tight junction barrier, ion transport, and inflammation. Gut **52:**439–451.
9. **Brunet, J. P., J. Cotte-Laffitte, C. Linxe, A. M. Quero, M. Geniteau-Legendre, and A. Servin.** 2000. Rotavirus infection induces an increase in intracellular calcium concentration in human intestinal epithelial cells: role in microvillar actin alteration. J. Virol. **74:**2323–2332.
10. **Brunet, J. P., N. Jourdan, J. Cotte-Laffitte, C. Linxe, M. Geniteau-Legendre, A. Servin, and A. M. Quero.** 2000. Rotavirus infection induces cytoskeleton disorganization in human intestinal epithelial cells: implication of an increase in intracellular calcium concentration. J. Virol. **74:**10801–10806.
11. **Chen, M. L., C. Pothoulakis, and J. T. LaMont.** 2002. Protein kinase C signaling regulates ZO-1 translocation and increased paracellular flux of T84 colonocytes exposed to *Clostridium difficile* toxin A. J. Biol. Chem. **277:**4247–4254.
12. **Ciarlet, M., and M. K. Estes.** 2001. Interactions between rotavirus and gastrointestinal cells. Curr. Opin. Microbiol. **4:**435–441.
13. **Cohen, C. J., J. T. Shieh, R. J. Pickles, T. Okegawa, J. T. Hsieh, and J. M. Bergelson.** 2001. The coxsackievirus and adenovirus receptor is a transmembrane component of the tight junction. Proc. Natl. Acad. Sci. USA **98:**15191–15196.
14. **Coyne, C. B., and J. M. Bergelson.** 2006. Virus-induced Abl and Fyn kinase signals permit coxsackievirus entry through epithelial tight junctions. Cell **124:**119–131.
15. **Coyne, C. B., T. Voelker, S. L. Pichla, and J. M. Bergelson.** 2004. The coxsackievirus and adenovirus receptor interacts with the multi-PDZ domain protein-1 (MUPP-1) within the tight junction. J. Biol. Chem. **279:**48079–48084.
16. **Cuadras, M. A., C. F. Arias, and S. Lopez.** 1997. Rotaviruses induce an early membrane permeabilization of MA104 cells and do not require a low intracellular Ca^{2+} concentration to initiate their replication cycle. J. Virol. **71:**9065–9074.

17. **Dickman, K. G., S. J. Hempson, J. Anderson, S. Lippe, L. Zhao, R. Burakoff, and R. D. Shaw.** 2000. Rotavirus alters paracellular permeability and energy metabolism in Caco-2 cells. Am. J. Physiol. Gastrointest. Liver Physiol. **279:**G757–G766.
18. **Feldman, G. J., J. M. Mullin, and M. P. Ryan.** 2005. Occludin: structure, function and regulation. Adv. Drug Delivery Rev. **57:**883–917.
19. **Fogh, J., J. M. Fogh, and T. Orfeo.** 1977. One hundred and twenty-seven cultured human tumor cell lines producing tumors in nude mice. J. Natl. Cancer Inst. **59:**221–226.
20. **Furuse, M., K. Fujimoto, N. Sato, T. Hirase, and S. Tsukita.** 1996. Overexpression of occludin, a tight junction-associated integral membrane protein, induces the formation of intracellular multilamellar bodies bearing tight junction-like structures. J. Cell Sci. **109:**429–435.
21. **Furuse, M., K. Fujita, T. Hiiragi, K. Fujimoto, and S. Tsukita.** 1998. Claudin-1 and -2: novel integral membrane proteins localizing at tight junctions with no sequence similarity to occludin. J. Cell Biol. **141:**1539–1550.
22. **Furuse, M., T. Hirase, M. Itoh, A. Nagafuchi, S. Yonemura, and S. Tsukita.** 1993. Occludin: a novel integral membrane protein localizing at tight junctions. J. Cell Biol. **123:**1777–1788.
23. **Gonzalez-Mariscal, L., A. Betanzos, and A. Avila-Flores.** 2000. MAGUK proteins: structure and role in the tight junction. Semin. Cell Dev. Biol. **11:**315–324.
24. **Gonzalez-Mariscal, L., A. Betanzos, P. Nava, and B. E. Jaramillo.** 2003. Tight junction proteins. Prog. Biophys. Mol. Biol. **81:**1–44.
25. **Gumbiner, B., T. Lowenkopf, and D. Apatira.** 1991. Identification of a 160-kDa polypeptide that binds to the tight junction protein ZO-1. Proc. Natl. Acad. Sci. USA **88:**3460–3464.
26. **Haskins, J., L. Gu, E. S. Wittchen, J. Hibbard, and B. R. Stevenson.** 1998. ZO-3, a novel member of the MAGUK protein family found at the tight junction, interacts with ZO-1 and occludin. J. Cell Biol. **141:**199–208.
27. **Hofman, P.** 2003. Pathological interactions of bacteria and toxins with the gastrointestinal epithelial tight junctions and/or the zonula adherens: an update. Cell. Mol. Biol. **49:**65–75.
28. **Ikenouchi, J., M. Matsuda, M. Furuse, and S. Tsukita.** 2003. Regulation of tight junctions during the epithelium-mesenchyme transition: direct repression of the gene expression of claudins/occludin by Snail. J. Cell Sci. **116:** 1959–1967.
29. **Jiang, B., L. Snipes-Magaldi, P. Dennehy, H. Keyserling, R. C. Holman, J. Bresee, J. Gentsch, and R. I. Glass.** 2003. Cytokines as mediators for or effectors against rotavirus disease in children. Clin. Diagn. Lab. Immunol. **10:**995–1001.
30. **Jourdan, N., J. P. Brunet, C. Sapin, A. Blais, J. Cotte-Laffitte, F. Forestier, A. M. Quero, G. Trugnan, and A. L. Servin.** 1998. Rotavirus infection reduces sucrase-isomaltase expression in human intestinal epithelial cells by perturbing protein targeting and organization of microvillar cytoskeleton. J. Virol. **72:**7228–7236.
31. **Kale, G., A. P. Naren, P. Sheth, and R. K. Rao.** 2003. Tyrosine phosphorylation of occludin attenuates its interactions with ZO-1, ZO-2, and ZO-3. Biochem. Biophys. Res. Commun. **302:**324–329.
32. **Klingler, C., U. Kniesel, S. D. Bamforth, H. Wolburg, B. Engelhardt, and W. Risau.** 2000. Disruption of epithelial tight junctions is prevented by cyclic nucleotide-dependent protein kinase inhibitors. Histochem. Cell Biol. **113:** 349–361.
33. **Kohler, K., D. Louvard, and A. Zahraoui.** 2004. Rab13 regulates PKA signaling during tight junction assembly. J. Cell Biol. **165:**175–180.
34. **Kovbasnjuk, O. N., U. Szmulowicz, and K. R. Spring.** 1998. Regulation of the MDCK cell tight junction. J. Membr. Biol. **161:**93–104.
35. **Lasala, C., D. Carre-Eusebe, J. Y. Picard, and R. Rey.** 2004. Subcellular and molecular mechanisms regulating anti-Mullerian hormone gene expression in mammalian and nonmammalian species. DNA Cell Biol. **23:**572–585.
36. **Latorre, I. J., M. H. Roh, K. K. Frese, R. S. Weiss, B. Margolis, and R. T. Javier.** 2005. Viral oncoprotein-induced mislocalization of select PDZ proteins disrupts tight junctions and causes polarity defects in epithelial cells. J. Cell Sci. **118:**4283–4293.
37. **Li, D., and R. J. Mrsny.** 2000. Oncogenic Raf-1 disrupts epithelial tight junctions via downregulation of occludin. J. Cell Biol. **148:**791–800.
38. **Lundgren, O., and L. Svensson.** 2001. Pathogenesis of rotavirus diarrhea. Microbes Infect. **3:**1145–1156.
39. **Mankertz, J., S. Tavalali, H. Schmitz, A. Mankertz, E. O. Riecken, M. Fromm, and J. D. Schulzke.** 2000. Expression from the human occludin promoter is affected by tumor necrosis factor alpha and interferon gamma. J. Cell Sci. **113:**2085–2090.
40. **Markou, T., M. Hadzopoulou-Cladaras, and A. Lazou.** 2004. Phenylephrine induces activation of CREB in adult rat cardiac myocytes through MSK1 and PKA signaling pathways. J. Mol. Cell. Cardiol. **37:**1001–1011.
41. **Martin-Latil, S., J. Cotte-Laffitte, I. Beau, A. M. Quero, M. Geniteau-Legendre, and A. L. Servin.** 2004. A cyclic AMP protein kinase A-dependent mechanism by which rotavirus impairs the expression and enzyme activity of brush border-associated sucrase-isomaltase in differentiated intestinal Caco-2 cells. Cell. Microbiol. **6:**719–731.
42. **Matter, K., and M. S. Balda.** 2003. Functional analysis of tight junctions. Methods **30:**228–234.
43. **Matter, K., and M. S. Balda.** 1999. Occludin and the functions of tight junctions. Int. Rev. Cytol. **186:**117–146.
44. **Matter, K., and M. S. Balda.** 2003. Signalling to and from tight junctions. Nat. Rev. Mol. Cell. Biol. **4:**225–236.
45. **Muza-Moons, M. M., E. E. Schneeberger, and G. A. Hecht.** 2004. Enteropathogenic *Escherichia coli* infection leads to appearance of aberrant tight junctions strands in the lateral membrane of intestinal epithelial cells. Cell. Microbiol. **6:**783–793.
46. **Nava, P., S. Lopez, C. F. Arias, S. Islas, and L. Gonzalez-Mariscal.** 2004. The rotavirus surface protein VP8 modulates the gate and fence function of tight junctions in epithelial cells. J. Cell Sci. **117:**5509–5519.
47. **Nusrat, A., C. A. Parkos, P. Verkade, C. S. Foley, T. W. Liang, W. Innis-Whitehouse, K. K. Eastburn, and J. L. Madara.** 2000. Tight junctions are membrane microdomains. J. Cell Sci. **113:**1771–1781.
48. **Nusrat, A., C. von Eichel-Streiber, J. R. Turner, P. Verkade, J. L. Madara, and C. A. Parkos.** 2001. *Clostridium difficile* toxins disrupt epithelial barrier function by altering membrane microdomain localization of tight junction proteins. Infect. Immun. **69:**1329–1336.
49. **Obert, G., I. Peiffer, and A. L. Servin.** 2000. Rotavirus-induced structural and functional alterations in tight junctions of polarized intestinal Caco-2 cell monolayers. J. Virol. **74:**4645–4651.
50. **Oswald, E., M. Sugai, A. Labigne, H. C. Wu, C. Fiorentini, P. Boquet, and A. D. O'Brien.** 1994. Cytotoxic necrotizing factor type 2 produced by virulent *Escherichia coli* modifies the small GTP-binding proteins Rho involved in assembly of actin stress fibers. Proc. Natl. Acad. Sci. USA **91:**3814–3818.
51. **Pinto, M., S. Robine-Leon, M. D. Appay, M. Kedinger, N. Triadou, E. Dussaulx, B. Lacroix, P. Simon-Assmann, K. Haffen, J. Fogh, and A. Zweibaum.** 1983. Enterocyte-like differentiation and polarization of the human colon carcinoma cell line Caco-2 in culture. Biol. Cell **47:**323–330.
52. **Quirin-Stricker, C., C. Mauvais, and M. Schmitt.** 1997. Transcriptional activation of human choline acetyltransferase by AP2- and NGF-induced factors. Brain Res. Mol. Brain Res. **49:**165–174.
53. **Rahn Landstrom, T., J. Mei, M. Karlsson, V. Manganiello, and E. Degerman.** 2000. Down-regulation of cyclic-nucleotide phosphodiesterase 3B in 3T3-L1 adipocytes induced by tumour necrosis factor alpha and cAMP. Biochem. J. **346:**337–343.
54. **Ramig, R. F.** 2004. Pathogenesis of intestinal and systemic rotavirus infection. J. Virol. **78:**10213–10220.
55. **Ruiz, M. C., J. Cohen, and F. Michelangeli.** 2000. Role of Ca^{2+} in the replication and pathogenesis of rotavirus and other viral infections. Cell Calcium **28:**137–149.
56. **Sakaguchi, T., H. Kohler, X. Gu, B. A. McCormick, and H. C. Reinecker.** 2002. *Shigella flexneri* regulates tight junction-associated proteins in human intestinal epithelial cells. Cell. Microbiol. **4:**367–381.
57. **Sakakibara, A., M. Furuse, M. Saitou, Y. Ando-Akatsuka, and S. Tsukita.** 1997. Possible involvement of phosphorylation of occludin in tight junction formation. J. Cell Biol. **137:**1393–1401.
58. **Servin, A. L.** 2003. Effects of rotavirus infection on the structure and functions of intestinal cells, p. 237–254. *In* U. Desselberger and J Gray (ed.), Viral gastroenteritis. Elsevier Science BV, Amsterdam, The Netherlands.
59. **Simonovic, I., J. Rosenberg, A. Koutsouris, and G. Hecht.** 2000. Enteropathogenic *Escherichia coli* dephosphorylates and dissociates occludin from intestinal epithelial tight junctions. Cell. Microbiol. **2:**305–315.
60. **Stevenson, B. R., J. D. Siliciano, M. S. Mooseker, and D. A. Goodenough.** 1986. Identification of ZO-1: a high molecular weight polypeptide associated with the tight junction (zonula occludens) in a variety of epithelia. J. Cell Biol. **103:**755–766.
61. **Tafazoli, F., C. Q. Zeng, M. K. Estes, K. E. Magnusson, and L. Svensson.** 2001. NSP4 enterotoxin of rotavirus induces paracellular leakage in polarized epithelial cells. J. Virol. **75:**1540–1546.
62. **Van Itallie, C. M., and J. M. Anderson.** 1997. Occludin confers adhesiveness when expressed in fibroblasts. J. Cell Sci. **110:**1113–1121.
63. **Wong, V.** 1997. Phosphorylation of occludin correlates with occludin localization and function at the tight junction. Am. J. Physiol. **273:**C1859–C1867.
64. **Wu, Z., P. Nybom, and K. E. Magnusson.** 2000. Distinct effects of *Vibrio cholerae* haemagglutinin/protease on the structure and localization of the tight junction-associated proteins occludin and ZO-1. Cell. Microbiol. **2:** 11–17.
65. **Yang, X., and G. Wand.** 2000. Ethanol uses cAMP-independent signal transduction mechanisms to activate proenkephalin promoter activity in rat C6 glioma cells. Alcohol Clin. Exp. Res. **24:**952–957.